JOURNAL OF THE AMERICAN WATER RESOURCES ASSOCIATION
Vol. 47, No. 3 AMERICAN WATER RESOURCES ASSOCIATION June 2011

CLIMATE CHANGE, ATMOSPHERIC RIVERS, AND FLOODS IN CALIFORNIA – A MULTIMODEL ANALYSIS OF STORM FREQUENCY AND MAGNITUDE CHANGES[1]

Michael Dettinger[2]

ABSTRACT: Recent studies have documented the important role that "atmospheric rivers" (ARs) of concentrated near-surface water vapor above the Pacific Ocean play in the storms and floods in California, Oregon, and Washington. By delivering large masses of warm, moist air (sometimes directly from the Tropics), ARs establish conditions for the kinds of high snowlines and copious orographic rainfall that have caused the largest historical storms. In many California rivers, essentially all major historical floods have been associated with AR storms. As an example of the kinds of storm changes that may influence future flood frequencies, the occurrence of such storms in historical observations and in a 7-model ensemble of historical-climate and projected future climate simulations is evaluated. Under an A2 greenhouse-gas emissions scenario (with emissions accelerating throughout the 21st Century), average AR statistics do not change much in most climate models; however, extremes change notably. Years with many AR episodes increase, ARs with higher-than-historical water-vapor transport rates increase, and AR storm-temperatures increase. Furthermore, the peak season within which most ARs occur is commonly projected to lengthen, extending the flood-hazard season. All of these tendencies could increase opportunities for both more frequent and more severe floods in California under projected climate changes.

(KEY TERMS: climate variability/change; meteorology; atmospheric rivers; flooding.)

Dettinger, Michael, 2011. Climate Change, Atmospheric Rivers, and Floods in California – A Multimodel Analysis of Storm Frequency and Magnitude Changes. *Journal of the American Water Resources Association* (JAWRA) 47(3):514-523. DOI: 10.1111/j.1752-1688.2011.00546.x

INTRODUCTION

Major floods are a recurring theme in California's climatology and hydrology, and have a long history of being an important cause of death and destruction in California (Kelley, 1998). Even today, California's aging water supply and flood protection infrastructure, including more than a thousand kilometers of levees, is challenged by punishing floods and increased standards for urban flood protection. Many Californians face unacceptable risks from flooding, both from where they live and work and from where they derive water supplies. In response to the risks and conflicts posed by flooding, the California Department of Water Resources Water Plan Updates in both 2005 and 2009 strongly recommend that water supply management and land-use development be much more fully integrated with flood management in the State (DWR, 2005, 2009). The Delta Vision Task

[1]Paper No. JAWRA-10-0049-P of the *Journal of the American Water Resources Association* (JAWRA). Received April 16, 2010; accepted December 20, 2010.

[2]Research Hydrologist, U.S. Geological Survey, Scripps Institution of Oceanography, 9500 Gilman Drive, Dept. 0224, La Jolla, California 92093 (E-Mail/Dettinger: mddettin@usgs.gov).

Force has identified improvements in floodplain and flood emergency management among its key recommendations for the future of California's Delta (Delta Vision Blue Ribbon Task Force, 2008). Perhaps most convincingly, the people of California passed Propositions 1E and 84 in 2006 to fund bonds intended to provide over $4.5 billion specifically for flood management programs in the State.

Although uncertainties abound, a significant part of this focus has been motivated by the risks that flood may occur more frequently or become more extreme with climate changes due to increasing greenhouse-gas concentrations in the global atmosphere. Current climate-change projections for 21st Century California uniformly include warming by at least a couple of degrees, and, although great uncertainties remain about future changes in long-term average precipitation rates in California (e.g., Dettinger, 2005; Cayan *et al.*, 2008), it is generally expected that extreme-precipitation episodes may become more extreme as the climate changes (Trenberth, 1999; Jain *et al.*, 2005; Cayan *et al.*, 2009). As a step toward better understanding of the risks and as an example of analysis of frequency changes in a specific storm and flood mechanism as a way of understanding likely overall flood frequency changes (Logan and Helsabeck, 2009), this paper summarizes a preliminary analysis of the 21st Century future of a particularly dangerous subset of flood-generating storms – the pineapple express or atmospheric-river storms – from seven current climate models.

CHARACTERISTICS OF ATMOSPHERIC-RIVER STORMS

Although warming alone may be expected to alter flood regimes in many snowfed settings by raising snowlines and increasing basin areas receiving rainfall in many storms (e.g., Knowles *et al.*, 2006; Dettinger *et al.*, 2009), changes in California's storm types, frequencies, or magnitudes may provide more direct and pervasive opportunities for change. Historically, the most dangerous storms in California have been warm and wet storms that strike in winter, producing intense rains over large areas and unleashing many of the State's largest floods. The most commonly recognized of these storms have been described as "pineapple express" storms because of the way that they are observed (in weather satellite and other imagery, e.g., Figure 1) to steer warm, moist air from the tropics near Hawaii northeastward into California (Weaver, 1962; Dettinger, 2004). More recently, studies have highlighted the fact that "pineapple express" storms in California are just one version of a more common feature of the midlatitude atmosphere (Dettinger *et al.*, 2011). It has been estimated that about 90% of all the water vapor transported toward the poles across the midlatitudes is transported within narrow, intense filamentary bands of moist air, called atmospheric rivers (ARs) (Zhu and Newell, 1998), that together typically span less than about 10% of the Earth's circumference at any given latitude. Ralph *et al.* (2006) recently noted that every "declared" flood on the Russian River near Guerneville, California, during the past 10 years has been associated with the arrival of an AR. Dettinger (2004) showed that, during the past >50 years, flows in the Merced River near Yosemite Valley have typically risen by about an order of magnitude more following the pineapple express form of ARs than following other winter storms. From these and other examples, AR storms are now increasingly understood to be the source of most of the largest floods in California, and an evaluation of the future of floods must attempt to understand their future.

The long thin band of high water-vapor amounts (yellow and orange) between roughly Hawaii and central California in Figure 1a, and the southwesterly band of (white) clouds in Figure 1b, is the AR associated with the New Year's 1997 storm (which yielded the flood of record on many California rivers) and gives a sense of the scope and scale of these features. The other panels show other ways of visualizing the same episode. Investigations by Ralph *et al.* (2004, 2006), Neiman *et al.* (2008a,b), and others have shown that, as they approach the west coast of North America, ARs are typically 2,000 or more kilometers long but only a few hundred kilometers wide (Ralph *et al.*, 2006). The air column within a typical AR will contain more than 2 cm of water vapor, with most of that vapor contained in the first 2.5 km above the sea surface and with a jet of intense and moist winds centered near about 2 km above the surface (Neiman *et al.*, 2008b). When the AR is oriented so that these intense winds carry their moist air directly up and over the mountains of California (i.e., in directions nearly perpendicular and upslope into the mountain ranges), intense storms of orographically enhanced precipitation result (Neiman *et al.*, 2002; Andrews *et al.*, 2004).

The presence or absence of ARs along the Pacific coast can be detected by monitoring the strength of the water-vapor transports across the region. The likely impact of such storms depends both on how much vapor the AR contains and how fast that vapor is being transported across coastal mountains where orographic uplift can extract the vapor as more or less intense precipitation. Intense pineapple express storms can be identified in daily general-circulation

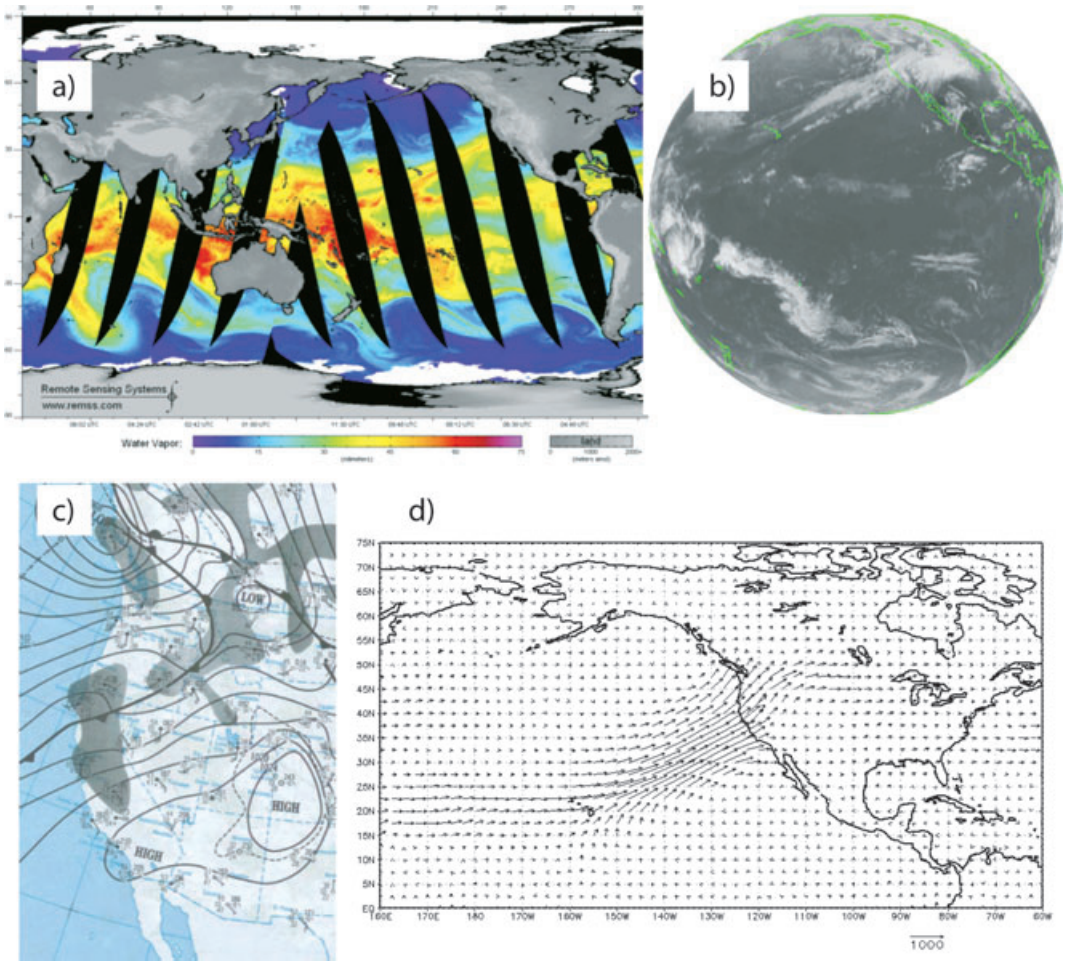

FIGURE 1. Various Approaches to Visualizing Atmospheric-River Conditions. SSM/I integrated water-vapor imagery from GMT morning on 2 January 1997 (a; warm colors for more vapor, cool colors for less), infrared weather-satellite imagery of the Pacific Ocean basin (GOES-West) from 18:00 hours GMT on 1 January 1997 (b; light colors are cloud bands, coasts indicated in green), corresponding daily weather map (c) and vertically integrated water-vapor transport directions and relative rates (d) from NCAR-NCEP Reanalysis fields; arrow at bottom indicates length of a 1,000 kg/m/s vapor-transport vector.

model (GCM)-scale atmospheric fields by tracing back to sources of intense water-vapor transport plumes to determine which begin in the subtropics or tropics near Hawaii (Dettinger, 2004). However, this can be a cumbersome algorithm to apply to current projections of climate change, because of the large fields that must be manipulated and because some of the necessary variables are not available from most of the IPCC GCMs at daily resolutions.

Thus, a more locally based strategy for detecting precipitation-rich AR-type storms along the California coast, designed and now being implemented for operational forecasting (Neiman *et al.*, 2009), is applied to climate-change projections from IPCC GCMs in the analysis presented here. The GCM-friendly AR-detection approach used here involves calculating the daily vertically integrated water vapor (IWV) in the atmosphere and daily wind speeds and directions at the 925-mb pressure level (about 1 km above the surface) for a GCM grid cell just offshore from the central California coast. In this study, these variables were determined for each day from the periods 1961-1980, 1981-2000, 2046-2065, and 2081-2100, and for a model-grid cell offshore from central California. These 20-year simulation periods are the only times for which daily water vapor, winds, and temperatures were available from six of the seven IPCC models addressed here (excepting only the GFDL GCM). The wind directions are evaluated to determine the component of wind that is directly upslope on the coastal mountain ranges in that vicinity, and when the upslope wind component is >10 m/s (vertical dashed line in Figure 2a) while the integrated water vapor is >2.5 cm (horizontal dashed line in Figure 2a), an AR storm is declared to be occurring. In nature, all storms that dropped more than 10 mm/hour of

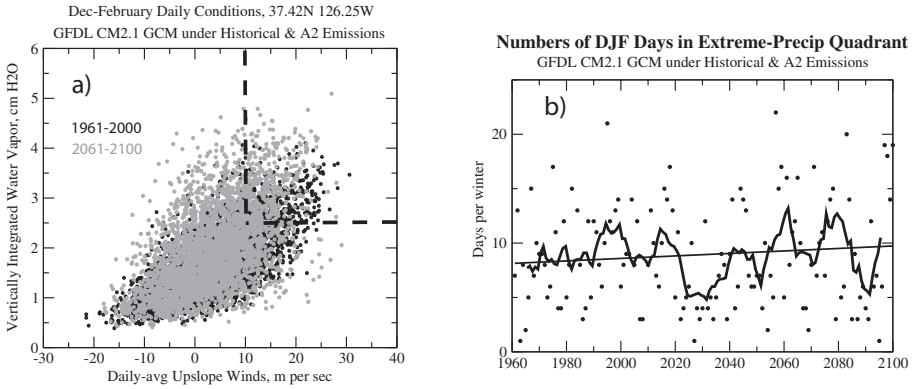

FIGURE 2. Plot of Daily December-February Integrated Water Vapor (IWV) and Upslope Wind Values From GFDL CM2.1 Climate Model (a) and Numbers of Days Per Winter Falling Into the Upper Right Quadrant of That Plot (b), Under Evolving 20th and 21st Century Climate Changes With A2 Greenhouse-Gas Emissions, Illustrate the Method of Detection of Atmospheric-River Conditions Used Here and an Example of How the Frequency of Atmospheric Rivers Varies Through Time. Thin straight line in panel (b) is a linear fit to data; thicker curve is a seven-year moving average of data.

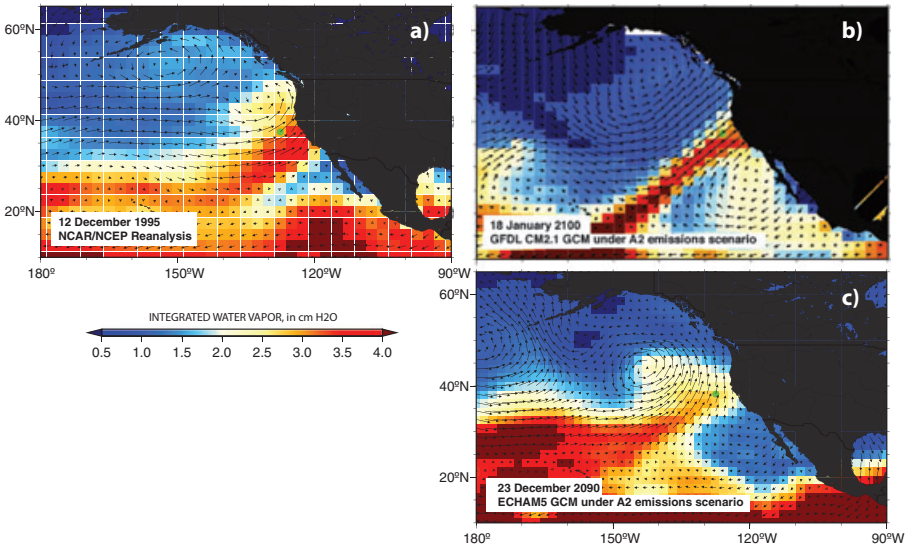

FIGURE 3. Maps of 925-mb Winds (vectors) and Integrated Water Vapor (shading) Over Oceans From (a) NCAR/NCRP Reanalysis Fields (updates to Kalnay *et al.*, 1996) on 12 December 1995, (b) the GFDL CM2.1 Climate Model Under an A2 Emissions Scenario on 18 January 2100, and (c) the Max-Planck Institute's ECHAM5 Climate Model Under the Same Emissions Scenario on 23 December 2090; Green Dots in Each Map Show the Location of the Grid Cell Used in the AR-Determinations Analyzed Here.

precipitation at the NOAA Cazadero meteorological station, in the Coastal Range north of San Francisco, in the past decade have met roughly these criteria. Applying the criteria above to historical and future climate simulations by seven IPCC GCMs allows us to compare the frequencies and magnitudes of AR storms arriving in California in the models under simulated historical and climate-changed conditions.

For example, Figure 3 shows wind vectors at the 925-mb pressure level (vectors) and integrated water vapor in the data-assimilated NCAR/NCEP Reanalysis depiction of the historical weather record (from updates to Kalnay *et al.*, 1996) (Figure 3a), and from two of the GCMs considered here (Figures 3b and 3c), on days that met the criteria of Figure 2a to be considered particularly intense ARs. All three maps show the long, narrow corridors of high-vapor content and strong upslope winds (approximately 40° north of westerly) previously illustrated in Figure 1 and characteristic of real-world ARs.

Neiman *et al.*'s (2009) approach to recognizing major storms on the West Coast is related to classical theory and methods for estimating precipitation based on general moisture convergences and fluxes in the atmosphere. Rasmusson (1967, 1968, 1971) analyzed large-scale atmospheric water-vapor transports

over North America to show the close and necessary relationships between vapor convergences and precipitation-minus-evaporation that form the basis of the atmospheric hydrologic cycle. Such considerations have since been developed to become important elements of understanding, forecasting, and modeling of precipitation (e.g., Banacos and Schultz, 2005; Evans and Smith, 2006).

The particular approach used here differs somewhat from most previous large-scale applications of atmospheric water balances to understand precipitation in that the most important impacts of ARs on West Coast precipitation come from their very local interactions with topography. Without topography and the orographic uplift of the air in ARs that they induce, the thousands of kilometers long, filamentary vapor transport represented by the ARs in their progress across the Pacific Ocean would continue on mostly uninterrupted. When the ARs make landfall, however, and encounter the mountain ranges of the Pacific Coast states, the warm, moist air that they contain is forced up to pass over the ranges. Upon uplift, large amounts of the uplifted vapor may be orographically rained out. Thus, the moisture convergence that gives the landfalling ARs their locally focused flood-generating power in California derives, not so much from large-scale atmospheric dynamics of fronts and convection, but rather from local orographic uplift (Neiman *et al.*, 2008b).

This distinction is particularly important in the context of trying to predict the future of these most dangerous of West Coast storms. Current GCMs represent processes, including orographic uplift, at coarse geographic resolutions (typically on order of several hundreds of kilometers at this latitude) and thus do not represent mountain ranges the size of the Sierra Nevada and Cascade Range as anything beyond the start of a gradual rise in topography from the West Coast toward the Rocky Mountains. The smaller coastal ranges of the Pacific Coast states are not present at all in current GCMs. As a consequence of this lack of topographic resolution, simulations of the most important storms affecting the West Coast lack the orographic-precipitation enhancements that account for most of the extreme precipitation that they might yield in the real world. Confronted with this missing element in current GCMs, and until much higher model resolutions become common, our primary avenue for inferring possible future changes in this most potent mechanism for flood generation is analysis of the AR conditions just offshore and just before they would, in the real world, have their flood-generating encounters with the first mountain ranges after many thousands of kilometers of passage over uninterrupted ocean surface. This limitation of current GCMs is the motivation, then, for the focus on just-offshore ARs of the present analysis.

PROJECTIONS OF ATMOSPHERIC-RIVER STORMS

As an example of the AR-identification procedure used here and the changes simulated by one particular climate model (GFDL CM2.1, from which complete daily data from 20th and 21st Centuries were available), a plot of daily IWV and upslope 925-mb wind speeds under GFDL CM2.1-simulated historical (heavy dots) and future 21st Century conditions (light dots) is shown in Figure 2a. Conditions on a relatively few historical December-February days fall in the upper right quadrant of this figure, where IWV >2.5 cm and upslope wind >10 cm, and the number of such days increases slightly as the climate evolves under the influence of increasing greenhouse-gas concentrations due to the A2 emissions scenario analyzed here (Figure 2b). The A2 emissions scenario is a scenario in which global greenhouse-gas emissions accelerate quickly throughout the 21st Century. This scenario is investigated here because it provides the strongest greenhouse forcing on climate, and thus the clearest indications of directions of change amidst natural variability, among the scenarios for which climate projections were commonly available in 2009. The slight increase in number of winter days that meet the historical AR criteria (in this particular model) is a suggestion that opportunities for major AR storms with potentially attendant winter flooding might increase with warming of the climate. In this model, the upslope winds slacken notably (light dots are generally farther left on Figure 2a than dark dots), perhaps due to general weakening of midlatitude westerly winds associated with weakening pole-to-equator temperature differences in the projections (Jain *et al.*, 1999). This slackening almost compensates for the tendency of the IWVs to be larger, so that only marginally more days appear in the "extreme-precipitation" upper right quadrant. By analyzing such figures from several models and by analyzing the corresponding projected vapor, wind, and temperature conditions that prevail on the days that meet the AR criteria, key factors that will determine the intensity and risks associated with individual AR events can be inferred.

The numbers of December-February days during the 1961-2000, 2046-2065, and 2081-2100 periods that have IWV >2.5 cm and upslope winds >10 m/s, in each of seven GCMs and in NCAR-NCEP Reanalysis (Kalnay *et al.*, 1996, and updates thereto), are

shown in Figure 4. The open (Reanalysis) diamonds represent real-world analogs to the simulated fields from the seven GCMs, and the number of Reanalysis AR episodes is on average lower than the numbers simulated by most of the GCMs (excepting the MIROC and MRI models). Nonetheless the range and general distribution of numbers of AR days per winter are not so different from the GCM counts as to preclude evaluations of the projected changes in the ensemble of GCM projections. Numbers of AR days during the 21st Century increase in most of the GCMs (compared to their respective historical counts). Most models simulate more winters with exceptionally large numbers of AR storms in the 21st Century, and fewer winters with exceptionally few such storms, so that changes in the frequency of these "extreme" winters are more notable than the changes in long-term mean numbers of AR storms.

To be more specific, Table 1 shows how the numbers of AR days per winter change through time on a model-by-model basis, as indicated by linear regressions of the AR-day counts from all available winters (1961-2000, 2046-2065, 2081-2100) *vs.* year. AR-day counts increase in five of the seven models and counts in the remaining models remain at historical levels. The projected increases in numbers of AR days in the 21st Century average about +2.5 days (across the ensemble of models), or by about 30%, by end of century. Thus, opportunities for winter-flood generating storms in central California are generally (but not unanimously) projected to increase in frequency in projections of climate change. No basic patterns or model differences exist between the GCMs that yield more ARs and those that do not, so that the current multimodel ensemble might best be interpreted as a random sampling of possible outcomes.

The intensity and characteristics of these simulated (and observed) AR events may also be evaluated, in order to determine how AR episodes themselves may evolve in the 21st Century. Figures 5 and 6 compare distributions of IWV values and upslope wind speeds on AR days under the historical

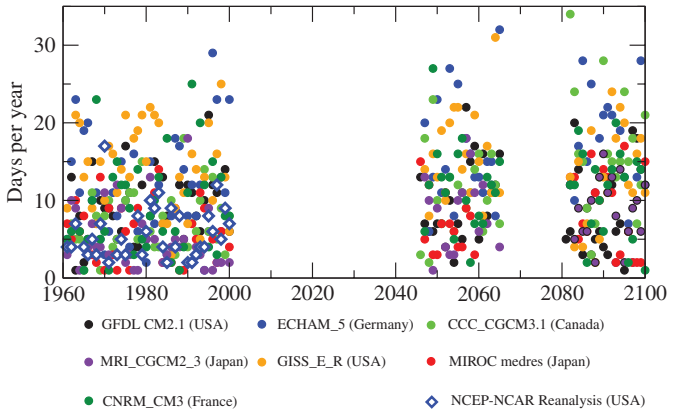

FIGURE 4. Numbers of December-February Days Per Year in the Upper Right Quadrant of Figure 2a, for Seven Climate Models (listed at bottom of figure) and the NCAR-NCEP Reanalysis Data Fields Illustrate Modest Increases in the Numbers of Atmospheric-River Storms Per Winter Through Time; 21st Century Counts Are From Projections Made in Response to A2 Emissions Scenarios.

TABLE 1. Trends in Numbers of AR Days/100 Years From Seven Climate Models, With Trends That Rise to Statistical Significance at 95% Level Highlighted in Boldface, and With (*) the Trend in CNRM at >90% Significance Level.

Climate Model	Change in # AR Days/100 Years	R^2 of Trend Fit (in %)
CCC	**+7.2 days**	**30**
CNRM	+2.4	4*
ECHAM	**+4.5**	**10**
GFDL	+0.4	0.2
GISS	+0.3	0
MIROC	**+2.2**	**7**
MRI	**+3.6**	**15**

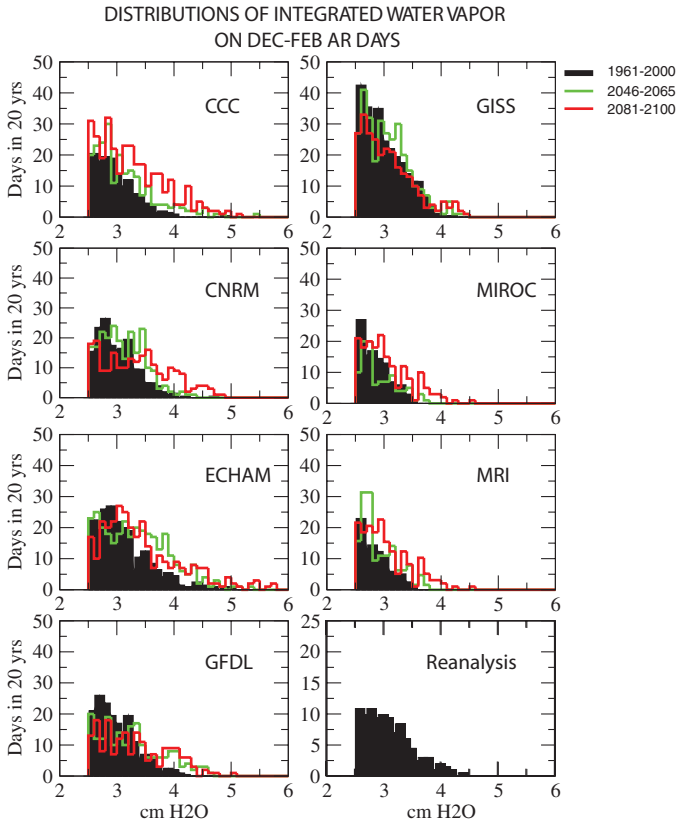

FIGURE 5. Histograms of Simulated Historical (assuming 20c3m-emissions, black) and Future (A2-emissions, green and red) Distributions of Integrated Water Vapor Values Associated With AR Days in Seven Climate Models and the NCAR-NCEP Reanalysis of Historical Observations Illustrate Increasingly Moist AR Conditions During the 20th and 21st Centuries.

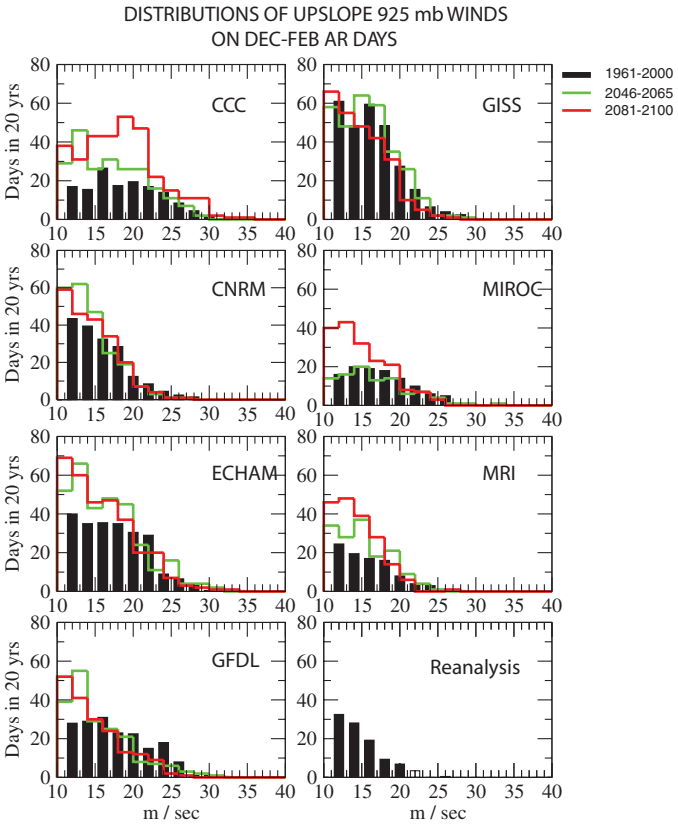

FIGURE 6. Same as Figure 5, Except for Upslope Winds on AR Days.

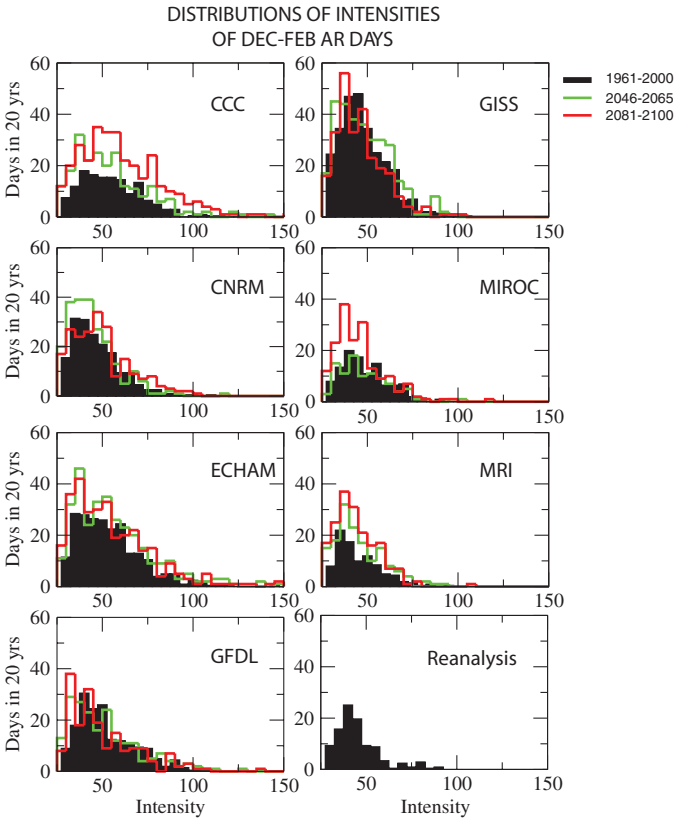

FIGURE 7. Same as Figure 5, Except for Intensities (IWV × upslope wind) on AR Days.

and projected future climates from each of the seven models and in the historical Reanalysis fields.

Integrated water vapor on AR days increases in all of the models, as do the numbers of AR days with IWV values greater than about 3.5-4 cm. In the real world, AR days with such high IWV values have been associated with the very largest storms (Neiman *et al.*, 2008a), and thus the increases at the rightmost edges of the histograms of Figure 5 could indicate rather ominous increases in the amount of precipitation that at least some of the AR days may deliver in the future.

On the other hand, the histograms of upslope wind speeds in Figure 6 indicate that, in all of the models except perhaps CCC, the upslope components of the winds transporting the additional water vapor tend to weaken as the 21st Century proceeds. These weaker upslope winds will tend to work against the increased water vapor to reduce the orographic-precipitation totals that the ARs might deliver.

The product of the upslope wind times the IWV gives an approximate sense of the water vapor delivered and available to be rained out of the AR storms as they pass over California's mountains. Figure 7 shows the distributions of this "intensity" product for each of the models, with the strong suggestion that in most models, although the numbers of AR days increase, the distributions of their overall intensities may not change as much. Table 2 shows the regressed trends for these intensities on a model-by-model basis, indicating that three of the seven models produce statistically significant increasing trends in the winter-average intensities of AR circulations, and two more models yield increases that are not statistically significant, while season-average intensities in the remaining two models remain more or less the

TABLE 2. Trends in Intensity (IWV × upslope wind speed) of AR Days/100 Years From Seven Climate Models, With Highlighting as in Table 1.

Climate Model	Change/100 Years	% Change/100 Years	R^2 (in %)
CCC	**+5.7 cm H_2O m/s**	**+11%**	**12**
CNRM	**+4.0**	**+9%**	**8**
ECHAM	**+3.8**	**+7%**	**6**
GFDL	+0.1	0	0
GISS	+1.6	+4	3
MIROC	−0.3	−1	0
MRI	+2.1	+5	3*

same. Even in the models that produce significant trends in AR intensity, the changes are not (on average) more than about 10%, which suggest average increases in rain from future AR storms on the order of +10%. Nonetheless, notice that more-than-historical numbers of ARs fall into the most intense tails of the projected distributions (Figure 7) from all seven GCMs. This tendency toward the occasional future occurrence of ARs that are more intense than any that have been witnessed historically is an indication that, as climate change proceeds, occasional AR storms may be exceptionally intense.

Atmospheric-river storms are associated with floods because of their relatively warm temperatures as well as the intense precipitation they can deliver. The warm temperatures associated with the ARs commonly result in elevated snowlines and thus much larger than normal river-basin areas receiving rain rather than snow. The long-term AR-day and all-day averages of surface-air temperatures from the entire ensemble of projections are shown in Figure 8 for the 1961-2000, 2046-2065, and 2081-2100 epochs. In the historical simulations, AR-day temperatures average 1.8°C warmer than the average of all December-February days, in close agreement with the observed (Reanalysis-based) average difference of 1.7°C. In the 21st Century simulations, both AR-day average temperatures and all-day average temperatures increase, by about +1°C in 2046-2065, and by about +2°C in 2081-2100. Notice that the AR-day average temperatures warm somewhat less quickly than all days, with all days warming by about 0.1°C more in 2046-2065 and by about 0.3°C more by 2081-2100. This modest difference in the rates of average warming presumably reflects the fact that ARs transport air from regions closer to the tropics, where overall rates of warming are projected to be less than in the midlatitudes (IPCC, 2007). Roughly, the +1.8°C warmer AR storms by the end of the 21st Century might be expected to lift snowlines by about 1.8°C* (1 km per +6.5°C warming) or +330 m on average, thereby increasing the average basin areas that receive rain rather than snow in many mountain settings.

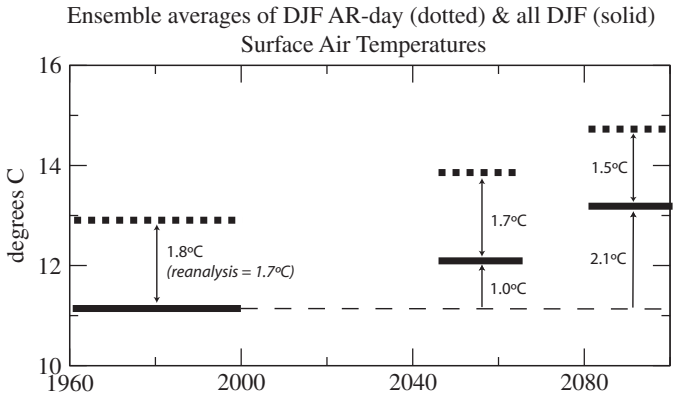

FIGURE 8. Ensemble Average Temperatures on December-February AR Days (dotted) and on All December-February Days (solid) Under Conditions Corresponding to Figures 5-7, Illustrate Increasing Temperatures During the 20th and 21st Centuries With Atmospheric River Days Warming Slightly Less Rapidly Than Winter Days in General.

Finally, the seasonality of AR days was investigated by counting the numbers of such occasions for each month of the year in the historical, 2046-2065, and 2081-2100 periods (not shown here; see Dettinger *et al.*, 2009). Generally speaking (with primary exception being the GFDL simulation), most of the increases in numbers of AR days under climate change occurred in the winter months, from about December to February. In five of the seven models, however, AR days also are projected to become notably more common in spring (CCC, GISS, MIROC, ECHAM, and MRI) and autumn (CCC, GISS, and MRI). Thus, there is a widely simulated potential for expansion of the season when AR storms occur. This may imply more potential for increased flooding before and after the primary historical flood season in California.

CONCLUSIONS

Atmospheric conditions associated with major storms and floods in California, in particular pineapple express or AR storms, were assessed here in the context of recent projections of 21st Century climate change. Projected changes in these storms are mostly at the extremes: Years with many AR storms become more frequent in most climate-change projections analyzed here, but the average number of such storms per year is not projected to change much. Likewise, although the average intensity of these storms is not projected to increase much in most models, occasional much-larger-than-historical-range storm intensities are projected to occur under the warming scenarios. Finally the AR storms warm along with, but not quite as fast as, the general mean temperatures in the seven projections analyzed.

The present analysis and results are limited, however, by the small ensembles of projections analyzed and by potential differences between simulated and real-world landfalling ARs. The multimodel ensemble approach presented here is an attempt to explore the range of possible climatic responses that might arise from the strong greenhouse forcings associated with the A2 emissions scenario used in all of the future climate projections included. Different models yield

different future AR statistics and ideally the spread among ensemble members would approximate our uncertainties about the climatic processes that might arise from the A2 emissions. However, a seven-member ensemble is relatively small and unlikely to reflect the full range of model uncertainties, and, beyond that limitation, our focus upon a single emissions scenario also does not address any of the uncertainties regarding future emissions (e.g., Dettinger, 2005). Finally, the 20-year time slices of simulated daily weather events compiled in the IPCC archives include only a couple of hundred AR events each and thus provide limited quantitative estimates of the changing statistics of ARs even among the GCMs sampled here. Thus, the present results remain preliminary and should be viewed more as qualitative indicators of the AR changes present in current climate-change projections, rather than as firm quantitative estimates of changed storm frequencies or characteristics. In order to arrive at more quantitative estimates, more simulations (realizations) of each time period from each model need to be made and archived, at daily levels, and an even wider range of climate models and emissions scenarios need to be included.

Nonetheless, the present results give indications that California flood risks from the warm-wet, AR storms may increase beyond those that we have known historically, mostly in the form of occasional more-extreme-than-historical storm seasons. More analysis is needed to increase understanding and certainties about this potential, but the analyses might serve as an example of how attention to details of how specific causes of flooding are projected to change (in this case, the frequency and magnitudes of AR storms) may provide early insights into how the overall risks of flooding may eventually change.

ACKNOWLEDGMENTS

Research described here was supported by both the California Energy Commission-funded California Climate Change Center and the CALFED Bay-Delta Program-funded Computational Assessments of Scenarios of Change in the Delta Ecosystem (CASCaDE) Project, and is in support of the California Energy Commission/NOAA/USGS CALWATER 2011 field campaign. These results were presented and discussed more fully in a report to the California Climate Action Team's 2008 biennial climate-change impacts assessment (Dettinger *et al.*, 2009).

LITERATURE CITED

Andrews, E.D., R.C. Antweiler, P.J. Neiman, and F.M. Ralph, 2004. Influence of ENSO on Flood Frequency Along the California Coast. Journal of Climate 17:337-348.

Banacos, P.C. and D.M. Schultz, 2005. The Use of Moisture Flux Convergence in Forecasting Convective Initiation: Historical and Operational Perspectives. Weather and Forecasting 20:351-366.

Cayan, D.R., E.P. Maurer, M.D. Dettinger, M. Tyree, and K. Hayhoe, 2008. Climate Change Scenarios for the California Region. Climatic Change 87(Suppl. 1):S21-S42, doi: 10.1007/s10584-007-9377-6.

Cayan, D., M. Tyree, M. Dettinger, H. Hidalgo, T. Das, E. Maurer, P. Bromirski, N. Graham, and R. Flick, 2009. Climate Change Scenarios and Sea Level Rise Estimates for California 2008 Climate Change Scenarios Assessment. California Energy Commission Report CEC-500-2009-014-D, Sacramento, California, 62 pp.

Delta Vision Blue Ribbon Task Force, 2008. Our Vision for the California Delta: Report to Governor Schwarzenegger, Sacramento, California, January 2008.

Dettinger, M.D., 2004. Fifty-Two Years of Pineapple-Express Storms Across the West Coast of North America. California Energy Commission PIER Energy-Related Environmental Research Report CEC-500-2005-004, Sacramento, California, 15 pp.

Dettinger, M.D., 2005. From Climate-Change Spaghetti to Climate-Change Distributions for 21st Century California. San Francisco Estuary and Watershed Science 3(1). http://repositories.cdlib.org/jmie/sfews/vol3/iss1/art4, *accessed* April 4, 2011.

Dettinger, M.D., H. Hidalgo, T. Das, D. Cayan, and N. Knowles, 2009. Projections of Potential Flood Regime Changes in California. California Energy Commission Report CEC-500-2009-050-D, Sacramento, California, 68 pp.

Dettinger, M.D., F.M. Ralph, T. Das, P.J. Neiman, and D. Cayan, 2011. Atmospheric Rivers, Floods, and the Water Resources of California. Water 3:455-478.

DWR (California Department of Water Resources), 2005. The California Water Plan Update 2005 – Highlights. DWR Bulletin 160-05. http://www.waterplan.water.ca.gov/docs/cwpu2005/cwphighlights/highlights.pdf, *accessed* April 4, 2011.

DWR (California Department of Water Resources), 2009. The California Water Plan Update 2009. Pre-Administrative Draft, DWR Bulletin 160-09, Chapter 7 – Implementation Plan. http://www.waterplan.water.ca.gov/cwpu2009/vol1/index.cfm, *accessed* April 4, 2011.

Evans, J.P. and R.B. Smith, 2006. Water Vapor Transport and the Production of Precipitation in the Eastern Fertile Crescent. Journal of Hydrometeorology 7:1295-1307.

IPCC (Intergovernmental Panel on Climate Change), 2007. Climate Change 2007–The Physical Science Basis. Cambridge University Press, New York, ISBN 978 0521 88009-1.

Jain, S., M. Hoerling, and J. Escheid, 2005. Decreasing Reliability and Increasing Synchroneity of Western North American Streamflow. Journal of Climate 18:613-618.

Jain, S., U. Lall, and M.E. Mann, 1999. Seasonality and Interannual Variations of Northern Hemisphere Temperature: Equator-to-Pole Gradient and Ocean–Land Contrast. Journal of Climate 12:1086-1100.

Kalnay, E., M. Kanamitsu, R. Kistler, W. Collins, D. Deaven, L. Gandin, M. Iredell, S. Saha, G. White, J. Woollen, Y. Zhu, A. Leetmaa, R. Reynolds, M. Chelliah, W. Ebisuzaki, W. Higgins, J. Janowiak, K.C. Mo, C. Ropelewski, J. Wang, R. Jenne, and D. Joseph, 1996. The NCEP/NCAR 40-Year Reanalysis Project. Bulletin of the American Meteorological Society 77:437-471.

Kelley, R., 1998. Battling the Inland Sea – Floods, Public Policy, and the Sacramento Valley. University of California Press, Berkeley, California, ISBN-13: 978-0520214286.

Knowles, N., M. Dettinger, and D. Cayan, 2006. Trends in Snowfall Versus Rainfall for the Western United States. Journal of Climate 19(18):4545-4559.

Logan, W.S. and L.J. Helsabeck, 2009. Research and Applications Needs in Flood Hydrology Science – A Summary of the October 15, 2008 Workshop of the Planning Committee on Hydrologic Science. National Academies Press, Washington, D.C., 34 pp. http://books.nap.edu/catalog/12606.html, *accessed* April 4, 2011.

Neiman, P.J., F.M. Ralph, A.B. White, D.A. Kingsmill, and P.O.G. Persson, 2002. The Statistical Relationship Between Upslope Flow and Rainfall in California's Coastal Mountains: Observations During CALJET. Monthly Weather Review 130:1468-1492.

Neiman, P.J., F.M. Ralph, G.A. Wick, Y.H. Kuo, T.K. Wee, Z. Ma, G.H. Taylor, and M.D. Dettinger, 2008a. Diagnosis of an Intense Atmospheric River Impacting the Pacific Northwest – Storm Summary and Offshore Vertical Structure Observed With COSMIC Satellite Retrievals. Journal of Applied Meteorology and Climatology 136:4398-4420, doi: 10.1175/2008MWR2550.1.

Neiman, P.J., F.M. Ralph, G.A. Wick, J.D. Lundquist, and M.D. Dettinger, 2008b. Meteorological Characteristics and Overland Precipitation Impacts of Atmospheric Rivers Affecting the West Coast of North America Based on Eight Years of SSM/I Satellite Observations. Journal of Hydrometeorology 9:22-47, doi: 10.1175/2007JHM855.1.

Neiman, P.J., A.B. White, F.M. Ralph, D.J. Gottas, and S.I. Gutman, 2009. A Water Vapor Flux Tool for Precipitation Forecasting. U.K. Water Management Journal (Special Issue on Weather Radar for Water Management) 162:83-94.

Ralph, F.M., P.J. Neiman, and G.A. Wick, 2004. Satellite and CALJET Aircraft Observations of Atmospheric Rivers Over the Eastern North-Pacific Ocean During the Winter of 1997/98. Monthly Weather Review 132:1721-1745.

Ralph, F.M., P.J. Neiman, G. Wick, S. Gutman, M. Dettinger, D. Cayan, and A.B. White, 2006. Flooding on California's Russian River – Role of Atmospheric Rivers. Geophysical Research Letters 33(L13801), 5 pp., doi: 10.1029/2006GL026689.

Rasmusson, E.M., 1967. Atmospheric Water Vapor Transport and the Water Balance of North America – Part I, Characteristics of the Water Vapor Flux Field. Monthly Weather Review 95:403-426.

Rasmusson, E.M., 1968. Atmospheric Water Vapor Transport and the Water Balance of North America – Part II, Large-Scale Water Balance Investigations. Monthly Weather Review 96:720-734.

Rasmusson, E.M., 1971. A Study of the Hydrology of Eastern North America Using Atmospheric Vapor Flux Data. Monthly Weather Review 99:119-135.

Trenberth, K.E., 1999. Conceptual Framework for Changes of Extremes of the Hydrological Cycle With Climate Change. Climatic Change 42:327-339.

Weaver, R.L., 1962. Meteorology of Hydrologically Critical Storms in California. Hydrometeorological Report No. 37, U.S. Department of Commerce, Washington, D.C.

Zhu, Y. and R.E. Newell, 1998. A Proposed Algorithm for Moisture Fluxes From Atmospheric Rivers. Monthly Weather Review 126:725-735.